RPE | Radiation Physics & Engineering
An International Peer-Reviewed Journal
Published by K.N. Toosi University of Technology
http://rpe.kntu.ac.ir
Research Article

Radiation Physics and Engineering 2021; 2(3):25–30
https://doi.org/10.22034/rpe.2021.302677.1038

# Dimensional analysis of high gradient RF cavity considering shrink-fit construction method

Mahdi Aghayan[a], S. Farhad Masoudi[a,*], Farshad Ghasemi[b], Hamed Shaker[c]

[a] *Department of Physics, K.N. Toosi University of Technology, P.O. Box 15875-4416, Tehran, Iran*
[b] *Physics and Particle Accelerators Research school, Nuclear Science and Technology Research Institute, Tehran, Iran*
[c] *Canadian Light Source, Saskatoon, Canada*

## HIGHLIGHTS

- A shrink-fit method is proposed for the construction high-gradient S-band cavity.
- Radiofrequency design of a 3-cell high gradient S-band cavity was performed.
- maximum gradient in the middle cell is twice that of the adjacent cells.
- Simulations showed maximum axial electric field of 59 MV.m$^{-1}$ is achievable for 2 MW input power.
- The breakdown rate less than $10^{-6}$ bpp.m$^{-1}$ is accessible for pulse length up to 80 $\mu$s.

## ABSTRACT

Advantage of non-brazing methods in manufacturing of cavities has been considered in high gradient studies because of the softening of copper by brazing cavities at high temperatures. Recent studies with hard copper cavities have been shown that the harder materials can reach larger accelerating gradients for the same breakdown rate. Shrinking, as a braze-free method for construction of the cavities, was used recently to fabricate and assemble acceleration cavities of an electron linear accelerator at the Institute for Research in Fundamental Science (IPM-Iran). Based on the results obtained in this project, this paper proposes the design of a 3-cell S-band standing wave structure operating at 2.9985 GHz for high gradient tests, considering shrink-fit construction method. The desired cavity consists of three cells so that the maximum gradient in the middle cell is about twice that of the surrounding cells. Simulation with Ansys-HFSS showed that maximum axial electric field 59 MV.m$^{-1}$ achievable for 2 MW input power in middle cell.

## KEYWORDS

High gradient linac
Shrinking construction method
Breakdown rate
RF design

## HISTORY

Received: 1 September 2021
Revised: 18 October 2021
Accepted: 31 October 2021
Published: Summer 2021

## 1 Introduction

Accelerating gradient in linacs is one of the main parameters that determines the cost and viability of these accelerators in various applications, such as linear colliders for high energy physics studies, electron sources of free electron lasers, and many medical and industrial applications. The S-band SLAC linac has an operating gradient of only about 17 MV.m$^{-1}$ (Neal and Blewett, 1970) while 100 MV.m$^{-1}$ gradient at 12 GHz has been considered in Compact Linear Collider (CLIC) at CERN (Simakov et al., 2018).

The major factor limiting the accelerating gradients is the vacuum RF breakdown phenomenon. It had been considered earlier that RF breakdowns to be directly related to the surface electric field (Wang and Loew, 1997; Balakin et al., 1978). Later, during the NLC and CLIC works, the statistical nature of the RF breakdown rate became apparent (Cahill et al., 2018; Wuensch et al., 2017). The breakdown rate (BDR) is one of the main quantitative requirements characterizing high gradient performance of RF cavities. Compact Linear Collider requires RF breakdown probability to be less than $4 \times 10^{-7}$ pulse$^{-1}$.m$^{-1}$ for accelerating gradient of 100 MV.m$^{-1}$. According to some recent studies (Simakov et al., 2018; Korsbäck et al., 2020; Dolgashev et al., 2020, 2018), to achieve higher accelerating gradients with lower RF breakdown rates (BDR), structures with hard copper alloys are preferred to the structures that made out of heat-treated ones. Using high temperature in brazing method causes softening the copper in the process. Therefore, non-brazing methods have been used for construction of high gradient structures.

*Corresponding author: masoudi@kntu.ac.ir

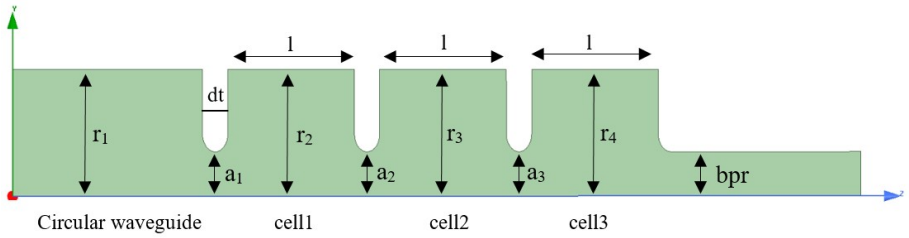


**Figure 1:** The three-cell cavity used for typical design.

A new fabrication technique for construction of high gradient S-band photogun has been recently developed and implemented at the Laboratories of Frascati of the National Institute of Nuclear Physics (INFN-LNF, Italy). Clamping method have been used for construction of high gradient S-band photogun and it was tested successfully at 120 MV.m$^{-1}$ (Alesini et al., 2018, 2015). Clamping method in combination with electron beam welding(EBW) and Tungsten Inert Gas (TIG) welding procedure have been employed in SLAC for construction of high gradient X-band single cell (Dolgashev et al., 2020, 2018). A novel technique of assembling the structure from milled halves has been used for a prototype 11.994 GHz, traveling-wave accelerating structure for the Compact Linear Collider (Argyropoulos et al., 2018). Reduction in cost, as well as a greater freedom in the choice of joining techniques are advantages of this technology. It might provide a way to produce a functional accelerating structure of hard copper. The procurement and testing of such a hard copper prototype structure is underway at CLIC (Korsbäck et al., 2020).

Shrinking as a braze-free method for construction cavities was used recently to fabricate and assemble acceleration cavities of electron linear accelerator at the Institute for Research in Fundamental Science (IPM-Iran) (Shaker et al., 2011; Ghasemi and Davani, 2015; Ghasemi et al., 2015; Hajari et al., 2018). The success of this method in the construction and assembling of the buncher and acceleration tube at IPM, led to the suggestion of using it for building high gradient cavities. Heat treatment does not used in shrinking method, so the copper structure remains hard and is expected to cause better performance in high gradient fields. There are some challenges in the construction of the cavity using this method, that need to be considered in the radio frequency and mechanical design. Since the sensitivity of high gradient cavity to the geometry is higher than low gradient cavity, it is more important to investigate the dimensional analysis.

In the present work, the design of a 3-cell S-band accelerating cavity is presented. Radiofrequency design has been performed with HFSS software in which electric and magnetic fields and modified Poynting vector have been employed to achieve optimal design.

## 2 Material and Methods

A typical design based on three cells has been considered for studying high gradient cavities. In this design, which is used to study the different materials and construction methods of high gradient cavity, a high gradient cell is considered between the first and last cells. In SLAC, this design has been used to evaluate the performance of high gradient X-band cavities. Different types of cavities have been constructed and tested with different materials, designs and construction methods in this center (Simakov et al., 2018; Cahill et al., 2018; Dolgashev et al., 2005, 2011, 2016, 2010). The main advantage of this method is the use of a small cavity instead of the actual multicell cavity, which significantly reduces construction costs. In this method, the structure is designed so that the input power is concentrated in the middle cell and therefore the axial field in the middle cell is the highest relative to the surrounding cells. In SLAC design, the axial field profile has been adjusted with changing the radius of the cells. The main feature of this design is the difference in radius of cells. Using this design for shrink-fit construction will cause the inner surface of the cylindrical waveguide to be stepped, which will reduce the high gradient capability. Therefore the radius of all cells was assumed to be the same in our design and the axial field profile can be adjusted only by changing iris radius.

Figure 1 shows the three-cell cavity used in a typical design. The primary dimensions of the cavity have been considered as $r_1 = r_2 = r_3 = r_4 = r = 40$ mm, $a_1 = a_2 = a_3 = bpr = 14$ mm, $l = 40$ mm and $dt = 8$ mm. The purpose of the design is to optimize the various dimensions of the cavity in order to achieve the following specifications:

1. 2998.5 MHz for the resonant frequency in the $\pi$ mode.
2. The highest value for axial field in the middle cell compare to the side cells.
3. The minimum reflection coefficient of the structure at resonance frequency.

Therefore, the effect of changing the dimensions of Fig. 1, on the resonant frequency and the axial electric field have been investigated. To investigate the effect of dimensional change on the axial field profile, the parameter "Relative Magnitude of E-Fields" was defined. This quantity gives the ratio of the maximum electric field in the first and third cells to the maximum electric field in the middle cell. Since one of the goals is to maximize the electric field in the middle cell, low value of this parameter is desirable in the design. To find the optimized dimensions, cavity simulations in Ansys HFSS electromagnetic

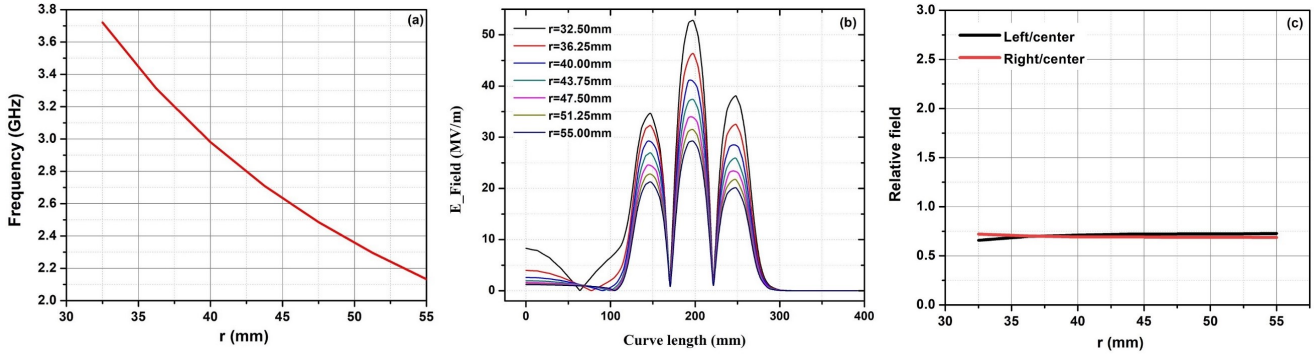


**Figure 2:** General desEffect of parameter $r$ on a) $\pi$ mode resonant frequency, b) axial E-Fields, and c) relative Magnitude of E-Fields.

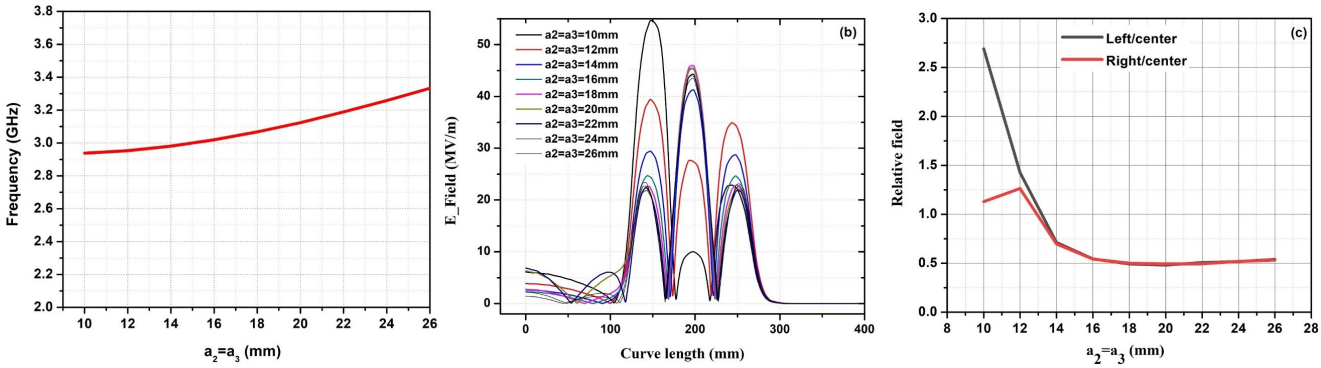


**Figure 3:** Effect of parameter $a_2 = a_3$ on a) $\pi$ mode resonant frequency, b) axial E-Field,s and c) relative Magnitude of E-Fields.

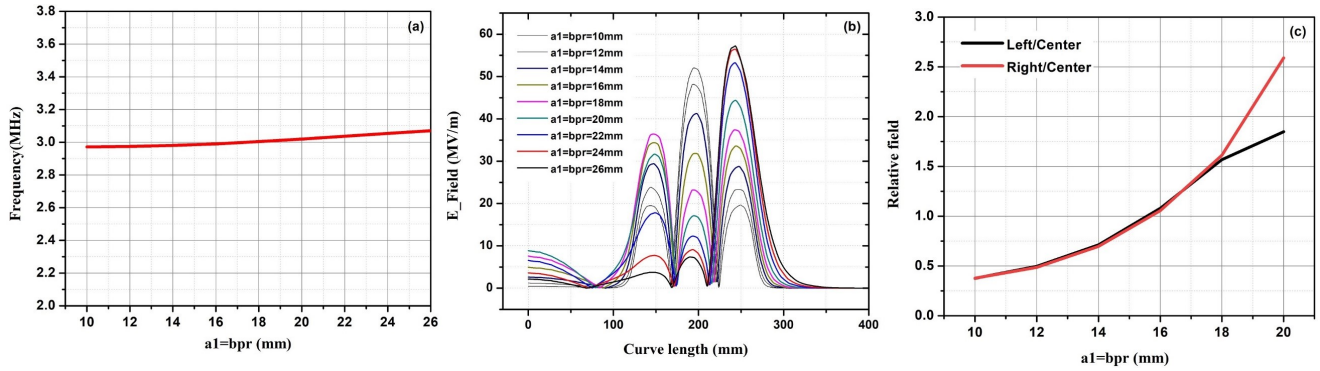


**Figure 4:** Effect of parameter $a_1 = bpr$ on a) $\pi$ mode resonant frequency, b) axial E-Fields, and c) relative Magnitude of E-Fields.

analysis software have been performed for seven different values of each parameter while the other parameters were fixed based on the primary values.

Another feature for testing the structure is the coupler which can be connected to the cavity with rf-compatible circular waveguide vacuum flanges. The flanges allow reuse of the same coupler for different structures, significantly reducing the cost of the experiments. The design of a suitable coupler for the desired cavity has been reported in the previous work (Aghayan et al., 2021).

## 3 Results and discussion

The resonant frequency, axial E-Fields and Relative Magnitude of E-Fields for different dimensions of Fig. 1 have been shown in Figs. 2 to 5.

It is seen in Figs. 2-a and 2-b that increasing the inner radius of the cavity, reduces the resonant frequency in the $\pi$ mode, as well as decreasing the axial E-Fields of the cavity. Figure 2-c shows that the change in internal radius has little effect on the Relative Magnitude of E-Fields.

The resonant frequency, axial E-Fields and Relative Magnitude of E-Fields for different values of $a_2$ and $a_3$ are shown in Fig. 3. As $a_2$ and $a_3$ are the iris radius of the discs that make up the middle cell and high gradient studies is performed in this cell, $a_2$ and $a_3$ need to be the same. As shown in Figure 3-a, increasing $a_2$ and $a_3$, increases the resonant frequency in the $\pi$ mode. It can be seen from Figs. 3-b and 3-c that $a_2$ and $a_3$ has a significant effect on the axial E-Fields. In the range $a_2$ and $a_3$ greater

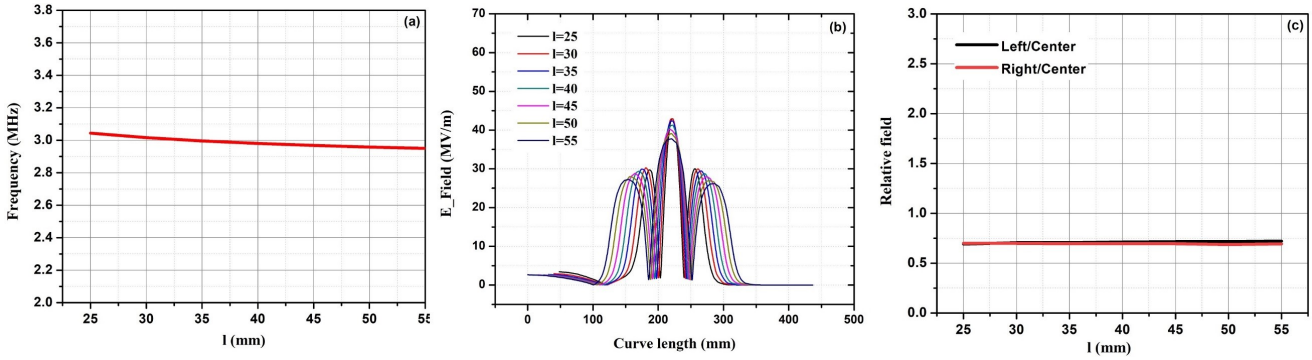


**Figure 5:** Effect of parameter $l$ on a) $\pi$ mode resonant frequency, b) axial E-Fields, and c) relative Magnitude of E-Fields.

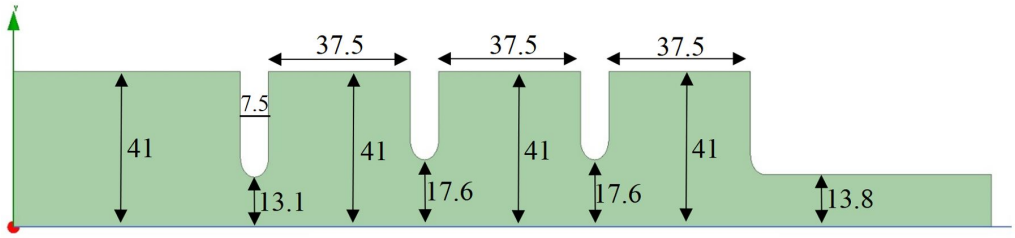


**Figure 6:** The structure of designed cavity with optimized parameters.

than 16 mm, relative magnitude of E-Fields is equal 0.5, which means the maximum axial E-Fields in the middle cell is twice that of the side cells, which is a good value for the designed cavity in this study.

Figure 4 shows the effect of $a_1$ and bpr on the resonant frequency, axial E-Fields and Relative Magnitude of E-Fields. To simplify the simulations, the values of $a_1$ and *bpr* were assumed to be the same. As shown in Figure 4-a, increasing $a_1$ and *bpr* increases the resonant frequency in the $\pi$ mode. However, comparing Figure 4-a and Figure 3-a, it can be seen that the effect of iris radii $a_2$ and $a_3$ on frequency is greater than the effect of radii $a_1$ and *bpr*. According to Figs. 4-b and 4-c, it is clear that increasing these parameters, reduces the axial field in the middle cell and increases in the side cells, which is not desirable in the design. Therefore, the values of these parameters need to be minimal.

Cavities with different $l$ values were simulated and the effect of $l$ value on the desired parameters were investigated in Fig. 5. As can be seen from Fig. 5-a, increasing the length of the cells reduces the resonant frequency in the $\pi$ mode. Figures 5-b and Figure 5-c show that increasing the cavity length has no effect on the Relative Magnitude of E-Fields.

By the results of Figs. 2 to 5, the radius has the greatest effect on the resonant frequency and by changing the iris radius, the axial E-Fields can be adjusted. For final design, by choosing appropriate radius, $\pi$ mode resonant frequency is set to 2988.5 MHz. Then, by changing $a_2$ and $a_3$, the axial electric field in the middle cell is adjusted two times greater than that of the surrounding cells. A change in the iris radius leads to change in the frequency. By changing the radius of the cells, $\pi$ mode resonant frequency is set to 2998.5 MHz again. After adjusting the axial electric field profile, the coupling between the cylindrical waveguide and the cavities must be tuned by changing the iris of the first cell. The final dimensions of the cavity are shown in Fig. 6.

The IPM electron linear accelerator laboratory in Iran has an RF test stand at frequency 2998.5 MHz based on 2 MW, KS237 klystron. Therefore, electric and magnetic fields have been calculated for 2 MW input power and are shown in Fig. 7 and Fig. 8, respectively. The maximum surface electric field in this power is 78 MV.m$^{-1}$ while maximum magnetic field is 113 kA.m$^{-1}$.

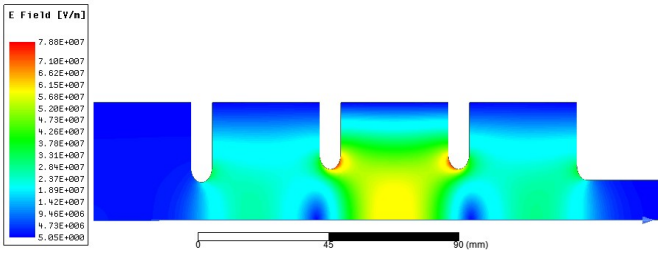


**Figure 7:** Electric field for 2 MW input power.

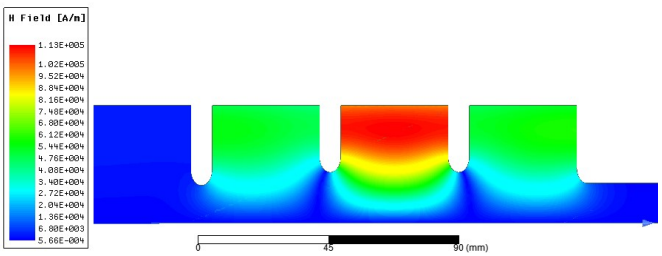


**Figure 8:** Magnetic field for 2 MW input power.

Figure 9 shows the axial electric field, reflection coefficient and VSWR for 2 MW input power. The maximum axial field in this power is equal to 59 MV.m$^{-1}$ in the middle cell, while in the first and third cells the maximum axial field are 28 and 30 MV.m$^{-1}$, respectively. The $S_{11}$ parameter shows a peak of $-45$ dB at the resonant frequency of 2998.5 MHz. Also, the value of VSWR at this frequency is equal to 1.01, which indicates a near critical coupling. Accelerating gradient is defined as $E_0T$, which $E_0$ is an average axial electric field and $T$ is transit-time factor (Simakov et al., 2018). By calculating the average field using Fig. 9-a data and also considering the transit-time factor equal to 0.8, the value of the accelerating gradient in the middle cell reaches 29 MV.m$^{-1}$ at 2 MW.

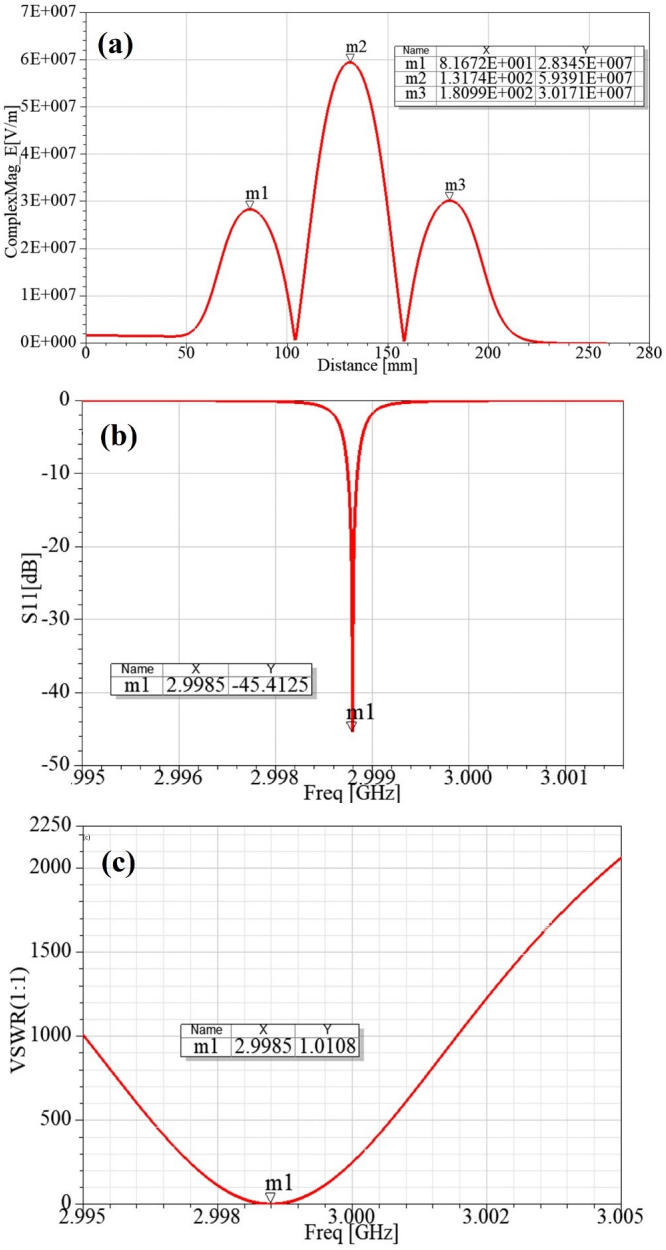


**Figure 9:** a) Axial electric field, b) reflection coefficient, and c) VSWR for 2 MW input power.

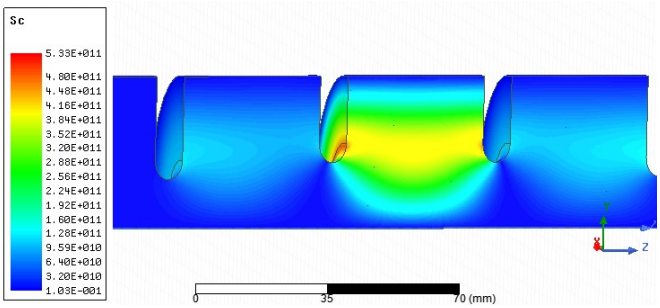


**Figure 10:** Modified Poynting vector ($S_c$) parameter for 2 MW input power.

One of the important parameters in high gradient studies is reaching the desired value for RF breakdown rate (BDR). In RF design, the modified Poynting vector ($S_c$) parameter has been used for studying RF breakdown rate. Based on experimental data from multiple cavities in CERN, its numerical value should not exceed 5 W.$\mu$m$^{-2}$ in order to have BDR less than $10^{-6}$ bpp.m$^{-1}$ at pulse length of 200 ns (Grudiev et al., 2009).

$S_c$ quantity has been formulated for the designed cavities in HFSS software and its diagram for 2 MW input power is shown in Fig. 10. The maximum value of this quantity is 0.53 W.$\mu$m$^{-2}$. By rescaling CLIC experimental data (5 W.$\mu$m$^{-2}$, 200 ns) using Eq. (1) (Benedetti et al., 2017), the pulse length can be increased up to 80 $\mu$s for BDR less than at 2 MW input power. But this test stand can also provide the mentioned power in 10 $\mu$s pulse length and 125 Hz repetition rate.

$$\frac{S_c^8\, t_p^3}{\mathrm{BDR}} = \mathrm{cons} \tag{1}$$

## 4 Conclusion

Radiofrequency design of a high gradient S-band cavity consist of cylindrical waveguide loaded by three discs (three cells) was performed. The effect of dimensional parameters of the cavity on the resonant frequency, axial E-Fields and Relative Magnitude of E-Fields was investigated. The axial electric field was adjusted so that the field in the middle cell became twice of the field in the surrounding cells. The simulations showed maximum axial electric field of 59 MV.m$^{-1}$ is achievable for 2 MW input power. Also, the study of the modified Poynting vector showed that for these input powers, the breakdown rate less than $10^{-6}$ bpp.m$^{-1}$ is accessible for pulse length up to 80 $\mu$s.

## Acknowledgment

Prof. Walter Wuensch, Head of the CLIC Project's high gradient cavity Group, is thanked for his valuable support and guidance in this research.

## References


Aghayan, M., Masoudi, S. F., Ghasemi, F., et al. (2021). Development of a novel approach for construction of high gradient braze-free s-band cavities. *Scientific Reports*, 11(1):1–13.

Alesini, D., Battisti, A., Bellaveglia, M., et al. (2018). Design, realization, and high power test of high gradient, high repetition rate brazing-free s-band photogun. *Physical Review Accelerators and Beams*, 21(11):112001.

Alesini, D., Battisti, A., Ferrario, M., et al. (2015). New technology based on clamping for high gradient radio frequency photogun. *Physical Review Special Topics-Accelerators and Beams*, 18(9):092001.

Argyropoulos, T., Catalan-Lasheras, N., Grudiev, A., et al. (2018). Design, fabrication, and high-gradient testing of an X-band, traveling-wave accelerating structure milled from copper halves. *Physical Review Accelerators and Beams*, 21(6):061001.

Balakin, V., Brezhnev, O., Novokhatskii, A., et al. (1978). Accelerating structure of a colliding linear electron-positron beam (VLEPP): investigation of the maximum attainable acceleration rate. Technical report.

Benedetti, S., Grudiev, A., and Latina, A. (2017). High gradient linac for proton therapy. *Physical Review Accelerators and Beams*, 20(4):040101.

Cahill, A., Rosenzweig, J., Dolgashev, V. A., et al. (2018). High gradient experiments with X-band cryogenic copper accelerating cavities. *Physical Review Accelerators and Beams*, 21(10):102002.

Dolgashev, V., Faillace, L., Higashi, Y., et al. (2020). Materials and technological processes for High-Gradient accelerating structures: new results from mechanical tests of an innovative braze-free cavity. *Journal of Instrumentation*, 15(01):P01029.

Dolgashev, V., Faillace, L., Spataro, B., et al. (2018). Innovative compact braze-free accelerating cavity. *Journal of Instrumentation*, 13(09):P09017.

Dolgashev, V., Gatti, G., Higashi, Y., et al. (2016). High power tests of an electroforming cavity operating at 11.424 ghz. *Journal of Instrumentation*, 11(03):P03010.

Dolgashev, V., Tantawi, S., Higashi, Y., et al. (2010). Geometric dependence of radio-frequency breakdown in normal conducting accelerating structures. *Applied Physics Letters*, 97(17):171501.

Dolgashev, V., Tantawi, S., Higashi, Y., et al. (2011). Status of high power tests of normal conducting single-cell structures. In *Conf. Proc. C0806233: mopp083, 2008*, number SLAC-PUB-14681. SLAC National Accelerator Lab., Menlo Park, CA (United States).

Dolgashev, V. A., Tantawi, S., Nantista, C., et al. (2005). RF breakdown in normal conducting single-cell structures. In *Proceedings of the 2005 Particle Accelerator Conference*, pages 595–599. IEEE.

Ghasemi, F. and Davani, F. A. (2015). Investigation of using shrinking method in construction of Institute for Research in Fundamental Sciences Electron Linear Accelerator TW-tube (IPM TW-Linac tube). *Journal of Instrumentation*, 10(06):P06011.

Ghasemi, F., Davani, F. A., Rachti, M. L., et al. (2015). Design, construction and tuning of S-band coupler for electron linear accelerator of institute for research in fundamental sciences (IPM E-linac). *Nuclear Instruments and Methods in Physics Research Section A: Accelerators, Spectrometers, Detectors and Associated Equipment*, 772:52–62.

Grudiev, A., Calatroni, S., and Wuensch, W. (2009). New local field quantity describing the high gradient limit of accelerating structures. *Physical Review Special Topics-Accelerators and Beams*, 12(10):102001.

Hajari, S. S., Haghtalab, S., Shaker, H., et al. (2018). RF emittance in a low energy electron linear accelerator. *Nuclear Instruments and Methods in Physics Research Section A: Accelerators, Spectrometers, Detectors and Associated Equipment*, 888:250–256.

Korsbäck, A., Djurabekova, F., Morales, L. M., et al. (2020). Vacuum electrical breakdown conditioning study in a parallel plate electrode pulsed dc system. *Physical Review Accelerators and Beams*, 23(3):033102.

Neal, R. B. and Blewett, J. P. (1970). The Stanford two-mile accelerator. *Physics Today*, 23(3):76.

Shaker, H. et al. (2011). Design of a Pi/2 Mode S-Band Low Energy TW Electron Linear Accelerator.

Simakov, E. I., Dolgashev, V. A., and Tantawi, S. G. (2018). Advances in high gradient normal conducting accelerator structures. *Nuclear Instruments and Methods in Physics Research Section A: Accelerators, Spectrometers, Detectors and Associated Equipment*, 907:221–230.

Wang, J. and Loew, G. (1997). Field emission and rf breakdown in high-gradient room temperature linac structures. Technical report, Stanford Univ., Stanford Linear Accelerator Center, CA (US).

Wuensch, W., Degiovanni, A., Calatroni, S., et al. (2017). Statistics of vacuum breakdown in the high-gradient and low-rate regime. *Physical Review Accelerators and Beams*, 20(1):011007.